NGU REPORT 2023.013

Hyperspectral imaging of cores from Heggdal, KBH1, E136 Vik–Julbøen
Mineral characterisation from hyperspectral imaging
Version 2: updated 25.10.2023

GEOLOGY FOR SOCIETY
SINCE 1858

GEOLOGICAL SURVEY OF NORWAY
· NGU ·

NORGES GEOLOGISKE UNDERSØKELSE
- NGU -

NGU REPORT
Geology for society

Geological Survey of Norway
P.O. Box 6315 Torgarden
NO-7491 Trondheim, Norway
Tel. +47 73 90 40 00

Report no.: 2023.013	**ISSN:** 0800-3416 (print) **ISSN:** 2387-3515 (online)	**Grading:** FORTROLIG / CONFIDENTIAL confidential to 01.03.2024	
Title: **Hyperspectral imaging of cores from Heggdal, KBH1, E136 Vik–Julbøen** Mineral characterisation from hyperspectral imaging Version 2, updated 25.10.2023			
Author: Tobias Kurz and Jasmin Schoenenberger		**Client:** Statens Vegvesen	
County: -		**Commune:** Vestnes (Møre og Romsdal)	
Map-sheet name (M=1:250.000): -		**Map-sheet no. & name (M1:50.000):** -	
Deposit name and grid-reference: -		**Number of pages:** 31 **Price (NOK):** - **Map enclosures:** -	
Fieldwork carried out: -	**Date of report:** 08/06/2023 Version 2: updated 25/10/2023	**Project no.:** 396800	**Person responsible:** Jochen Knies

Summary

This report summarises the results from the pilot project with Statens Vegvesen to evaluate the potential for mineral characterisation and to map and quantify clay minerals with swelling potential in drill cores using hyperspectral imaging. Eight core boxes from the Heggdal core KBH1, drilled for the infrastructure project E136 Vik–Julbøen (Vestnes, Møre og Romsdal) have been selected. The core boxes have been scanned with the core hyperspectral imaging system at NGU using a SisuRock scanning system equipped with two hyperspectral image cameras measuring within the visible near-infrared (VNIR, 400-1000nm) and short-wave infrared (SWIR, 1000-2500nm) spectral range.

The evaluation of the hyperspectral image data shows that image spectra with smectite and chlorite signatures have been found. The spectra and spectral maps indicate that the clay composition in these cores is dominated by smectite and chlorite and both minerals are found in all core boxes. Spectrally highest smectite concentration have been found at core depth 348.65-349.00m and spectrally highest chlorite concentrations have been found at 1134.65-1135.00m. The spectral mapping results can guid sampling and swelling pressure should be tested at these spots.

XRD analysis confirms that spectra interpreted to be representative of smectite and chlorite in these data showing highest concentrations of these minerals and that the clay mineral composition in these cores are dominated by smectite and chlorite. The XRD analysis also indicates that the spectral maps provide representative mineral distribution and abundance (sub-pixel concentration) maps.

This study confirms the potential of core hyperspectral imaging for mineral characterisation and to map minerals of particular interest such as swelling clays or other hazardous material over the entire core lengths. Following up projects are recommended for more comprehensive confirmation studies, to determine limitations and to adjust the method for the need for infrastructure projects.

Keywords

Hyperspectral imaging	Core logging	Swelling clay
Basement weathering	Heggdal	E136 Vik–Julbøen

Geological Survey of Norway
P.O. Box 6315 Torgarden
NO-7491 Trondheim, Norway
Tel. +47 73 90 40 00

NGU project report

Hyperspectral imaging of cores from Heggdal, KBH1, E136 Vik–Julbøen

- Mineral characterisation from hyperspectral imaging –

GEOLOGICAL SURVEY OF NORWAY
- NGU -

Authors:

Dr Tobias Kurz and **Dr Jasmin Schoenenberger**

tobias.kurz@ngu.no
jasmin.schonenberger@ngu.no
Geological Survey of Norway, Trondheim, Norway

Date of issue: 08/06/2023, version 2: 25/10/2023
Document version: **2.0**

Report prepared for Statens Vegvesen
Contact in Statens Vegvesen: Torkild Åndal
torkild.aandal@vegvesen.no

Confidentiality:
Report accessible for third parties from February 2024, with the consent of Statens Vegvesen.

Table of contents

Abbreviations

c.	circa
DSLR	digital single-lens reflex
HSI	hyperspectral imaging
LWIR	long wave infrared
NGU	Norges Geologiske Undersøkelse
MSc	Masters of Sciences
RGB	red, green, blue
SVV	Statens Vegvesen
SWIR	short wave infrared
VNIR	visible near infrared
XRD	X-ray diffraction

1. PROJECT AND REPORT AIM

The motivation of this small-scale pilot-project (11 working days) was to measure eight core boxes (circa 40m core length) from the Heggdal cores (KBH1, E136 Vik – Julbøen) using core hyperspectral imaging (HSI) for mineral characterisation. The project aims to evaluate the potential of HSI to identify, map and quantify swelling clays in core material. The analysed core boxes are listed and shown in table 1 and figure 1. According to the project agreement, the results should be presented in an oral presentation, however SVV could not suggest a suitable meeting date. The report briefly summarises the main results and findings from the HSI and mineral analysis to finalise this project but do not provide detailed technical information about the processing and data evaluation. Several additional analysis methods and spectral mapping products have been carried out and used for the data exploitation. Not all methods and products are shown in this report.

Table 1. Selected core boxes used in this project from Heggdal core KBH1, E136 Vik–Julbøen.

Box number in this project	Core name	Core ID	Depth from	Depth to
1	Heggdal	KBH1	345	350
2	Heggdal	KBH1	355	360
3	Heggdal	KBH1	765	770
4	Heggdal	KBH1	870	875
5	Heggdal	KBH1	945	950
6	Heggdal	KBH1	1030	1035
7	Heggdal	KBH1	1055	1060
8	Heggdal	KBH1	1130	1135

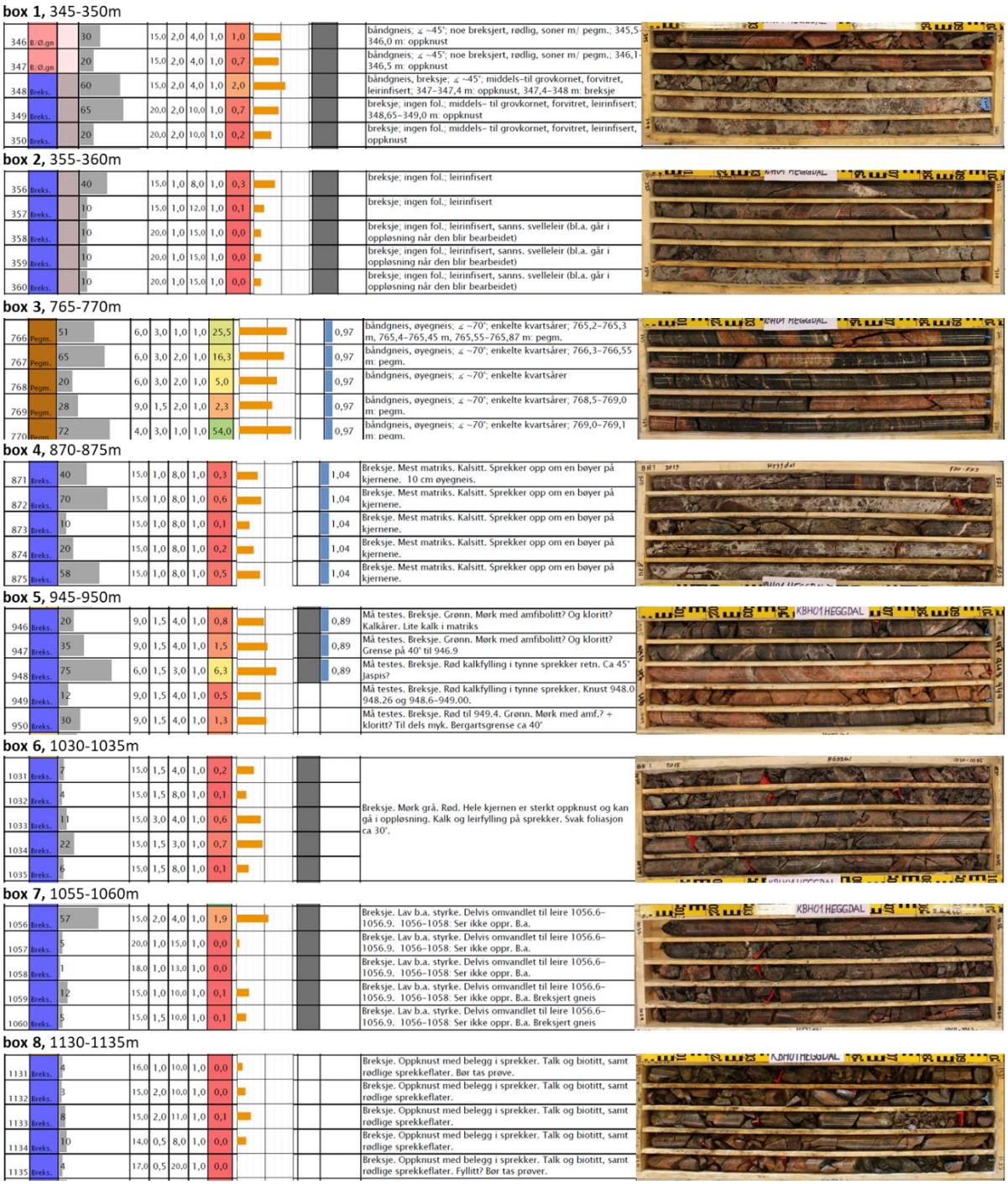

Figure 1. Core logs from SVV from the core boxes used in this project.
Source: Kjernelogg KBH 01 Heggdal, E136 Vik – Julbøen, Statens Vegvesen, PDF dokumenter.

Background

Specific clay minerals can show expansive properties when absorbing water. Mainly clay minerals belonging to the smectite mineral group such as montmorillonite or nontronite possess high swelling potential. However, also mixed-layer clays such as chlorite-smectite, illite-smectite, kaolinite-smectite and others can form expandible interlayers due to smectite layers. Thus, mixed-layers clays can also possess swelling potential. Beside other petrophysical properties, mineral composition and concentration of swelling clay mineral types are controlling factors of the swelling pressure for example in weakness zones in basement rocks. Hyperspectral imaging is a non-destructive and image-based method to analyse mineral composition based on diagnostic reflectance and absorption properties and allow to semi-quantify mineral composition in sample or core material. HSI is capable to detect and differentiate between different clay mineral types and can be used for example to identify and map clay minerals with swelling potential such as smectite. Kurz et al. (2017) has shown in a prove of concept study, commissioned by Statens Vegvesen, the potential of HSI to indicate swelling potential from sample material from different weakness zones within the Svegatjørn–Rådal tunnel (E39 in Bergen). In this study sample materials with known swelling pressure have been analysed with HSI to determine the mineral composition of these samples. The concentration of smectite derived from HSI indicated a correlation with the swelling pressure. In this present project, HSI is tested on selected core boxes for mineral characterisation and to identify material with swelling potential within the Heggdal cores (KBH1, E136 Vik - Julbøen)

Spectral properties of relevant material

Clays minerals show diagnostic absorption features due to hydroxyl-ions at 1400nm and 2200nm and due to water molecules at 1900nm. Spectral properties such as the exact wavelength positions (see Appendix B), the shapes of the absorption features, occurrence of double minima or the shape of the entire spectral curve and other reflectance properties allow to differentiate between different clay types such as smectite, illite, chlorite, kaolinite, and others (Figure 2). HSI allows also to determine, to some extent, specific members of these mineral groups.

Many tectosilicates such as quartz and feldspar do not have diagnostic absorption features within the measured visible near-infrared (VNIR) and short-wave infrared (SWIR) spectral range. For more reliable identification and differentiation between, for example different feldspar types, the long wave infrared (LWIR) spectral range is required. Spectra of pure quartz and feldspar are commonly featureless (flat curves) within VNIR-SWIR light. However, impurities, intracrystalline water molecules or alteration processes can cause absorption features for these minerals. Thus, spectra from quartz or feldspar-rich rocks might be differentiable, due to the flat curve shape, to some extend in contrast to the other material present in this specific data set.

When evaluating a spectral data set it can be also of relevance when diagnostic absorption features have not been observed which than indicates the absent of specific minerals. For example, in this present data set no double minima at 1400 and 2200nm has been observed, indicating the absence of kaolinite.

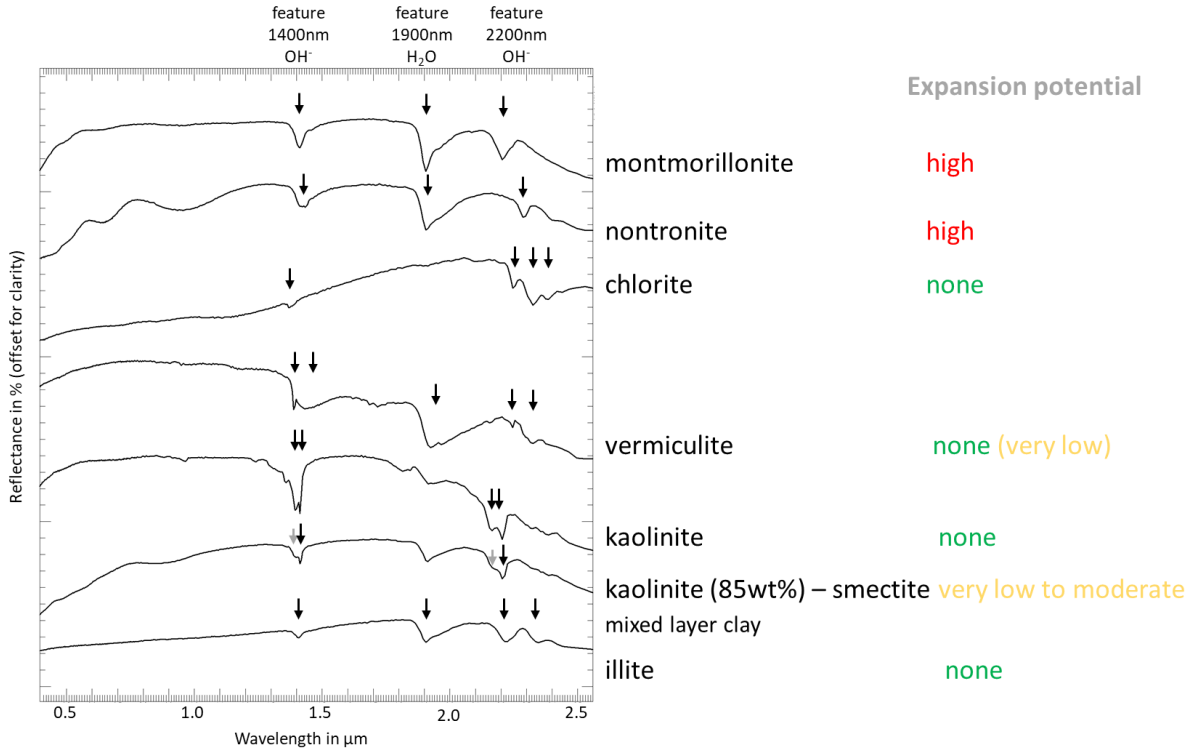

Figure 2. Examples of reflectance spectra of clay minerals form the USGS spectral library (Clark et al. 2003). Arrows indicating diagnostic absorption features.

2. DATA COLLECTION

The core boxes have been selected from different core depths to cover diverse and representative lithology and mineralogy. The core boxes have been scanned at NGU (31. January 2022) with a SisuRock core scanning system equipped with two hyperspectral cameras (Table 2, Figure 3). One camera measuring within the visible and near-infrared spectral range (VNIR, 350-1000nm) and the other measuring within the short wave infrared spectral range (SWIR, 1000-2500nm). Diagnostic absorption properties of clay minerals occur particularly within the SWIR spectral range. The scanning settings have been chosen to ensure a pixel resolution of c.1mm for the hyperspectral images in both spectral ranges. Additionally, the core boxes have been photographed with a dry and wetted surface using a full frame high resolution DSLR camera.

Figure 4 shows the photographs, the VNIR and SWIR imagery and the box numbering used in this project. Please note that the core boxes come from different core depths and the right upper corner in the boxes are the tops. Box sections are therefore counted from right (section1) to left (section 5). The spectral diagrams at the left side of figure 4 indicate the spectral ranges of the VNIR and SWIR images and which spectral bands have been used to visualise the hyperspectral images in red, green, and blue (RGB).

Pixels not containing any geological information have been excluded from processing by generating image masks (Figure 5B), only white pixels in figure 5B are included in the processing. Figure 5C shows an auto-classification (also termed unsupervised classification or segmentation) using K-means classification with 10 classes. Such auto-classification does not require any previous material information in the imagery and requires very little user input. It is segmenting the dataset by statistical parameters only. This is an efficient way to get initial information about spectral differences or similarities in the dataset. Depending on the mathematical methods chosen, auto-classification often does not reveal all spectral details and often overlooks material present in small quantities, but proving an initial spectral mapping product which can be useful to identify areas of interest and can be used for initial geological interpretation.

Table 2. Main specification of the hyperspectral cameras.

	VNIR camera	SWIR camera
Spectral range	400-1000 nm	1000-2500 nm
Max number of spectral bands	946	288
Band sampling	0.6 - 5.0 nm	6 nm
Number of pixels in scan line	2184	384
Digital resolution	16 bit	16 bit

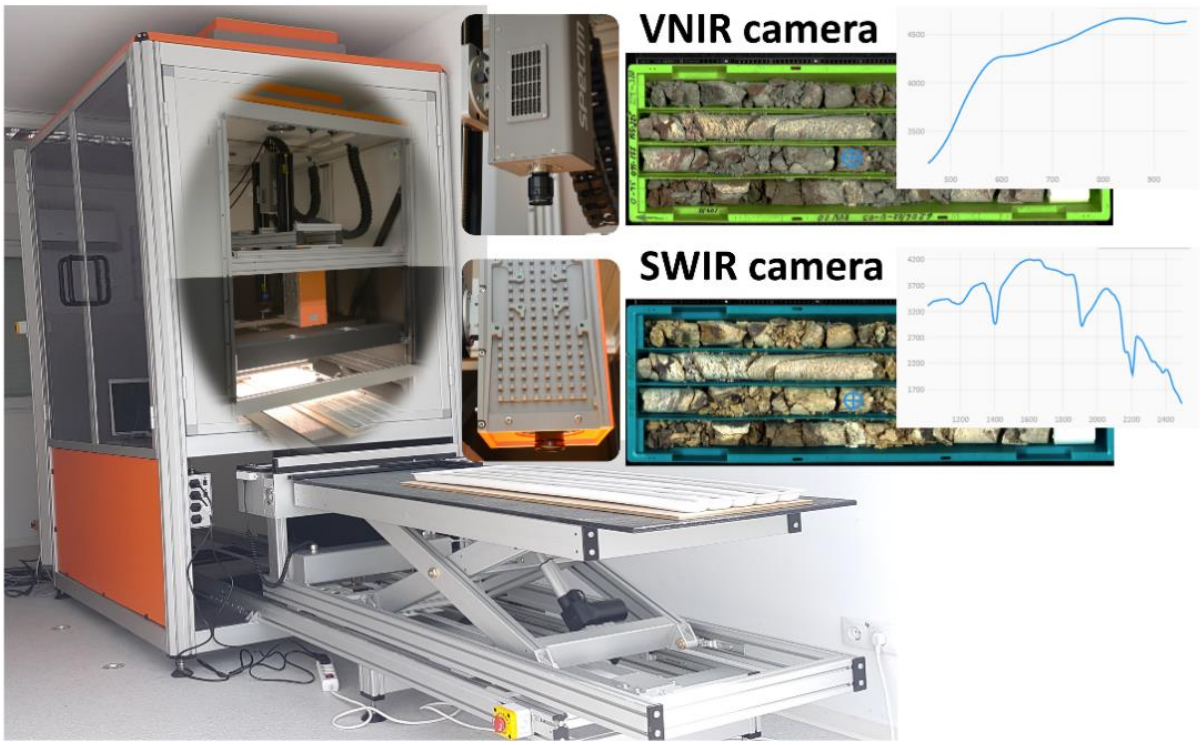

Figure 3. SisuRock core scanning system at NGU equipped with two hyperspectral cameras.

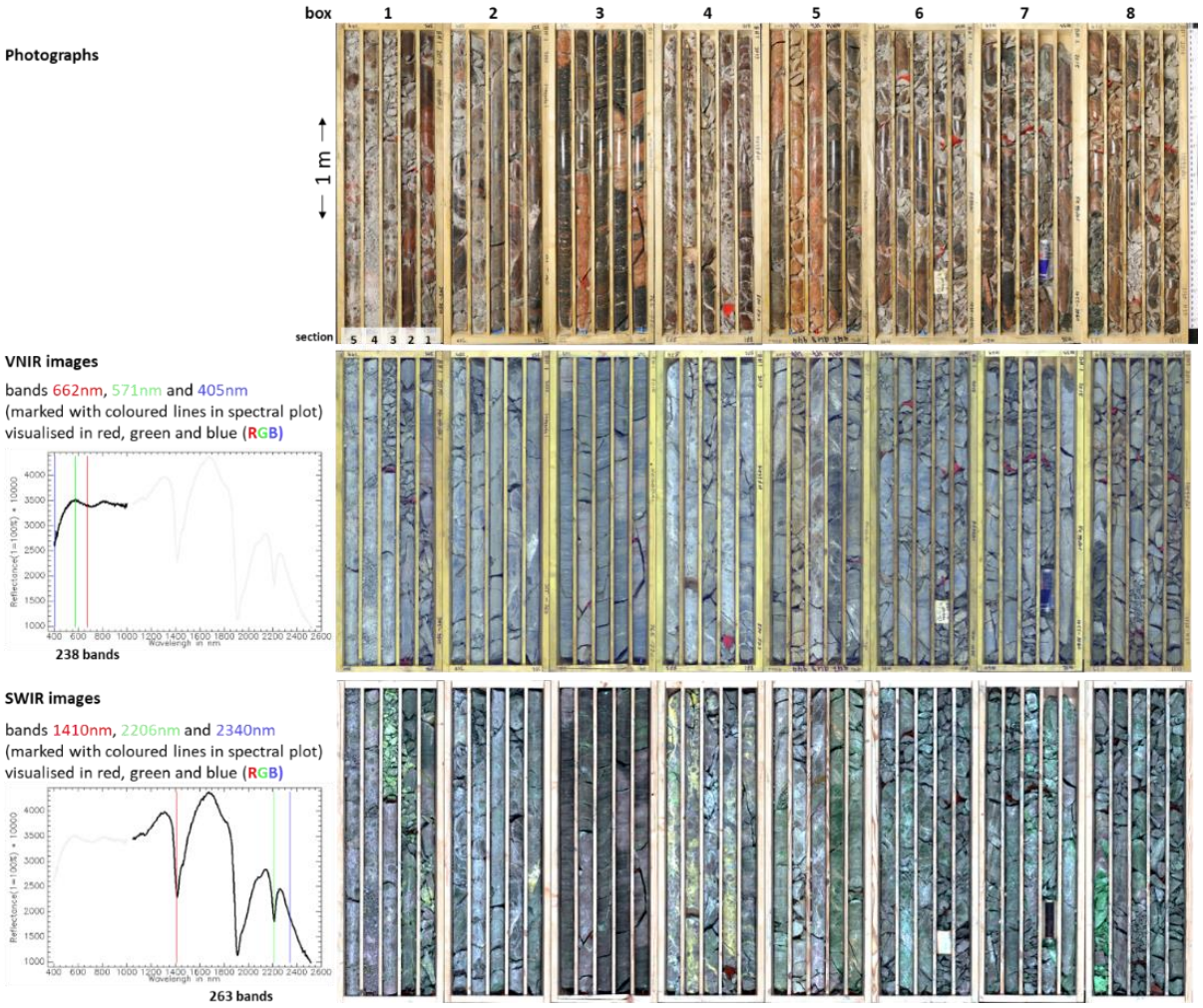

Figure 4. Photographs, VNIR and SWIR hyperspectral images of the core boxes. Boxes are numbered from 1 to 8 for this project. Note: boxes are from different core depths of core KBH1, E136 Vik - Julbøen (see Table 1). The right upper corner in the boxes are the tops. Box sections are therefore counted from right (section1) to left (section 5). Core diameter is c.4.5cm.

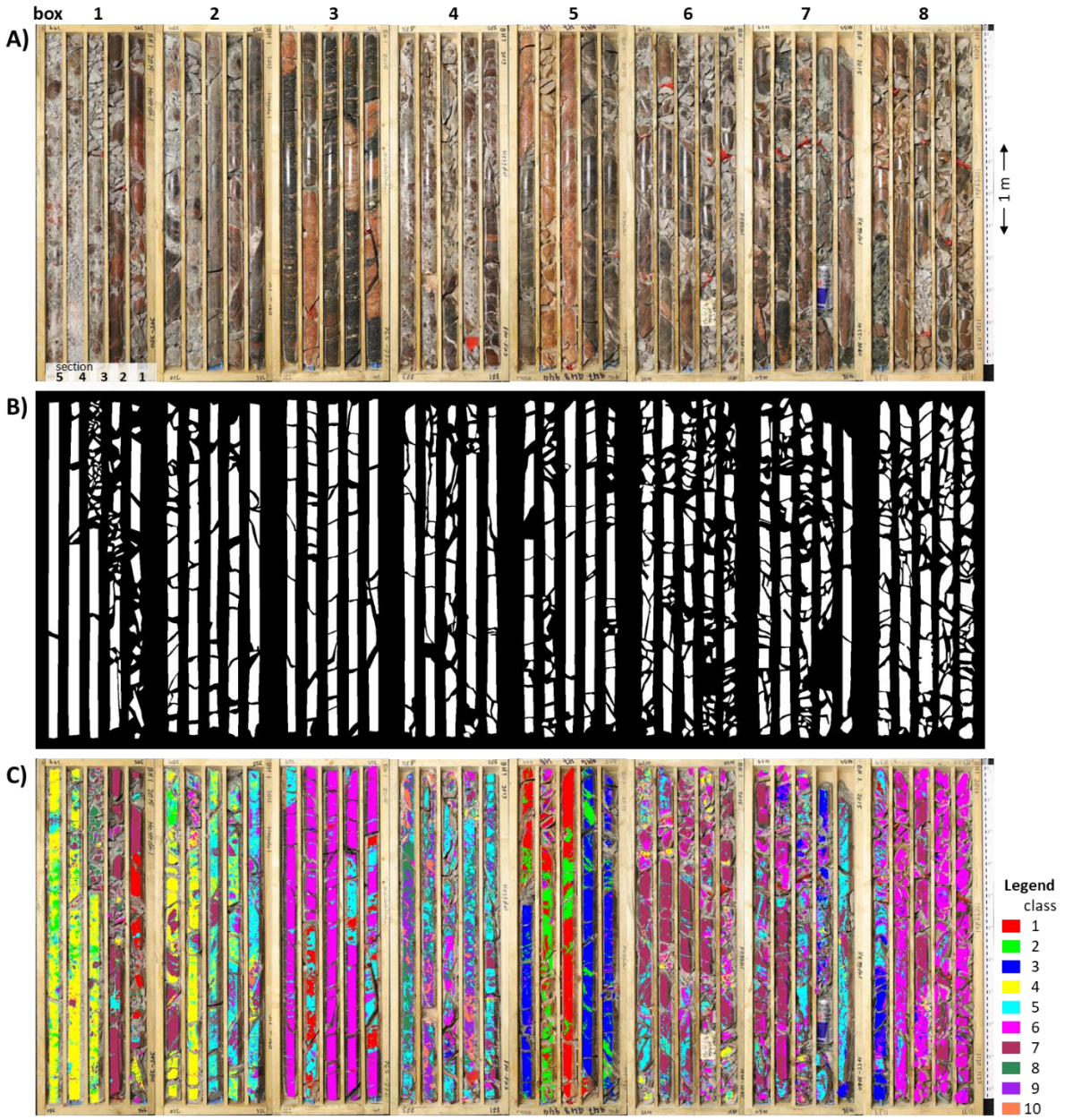

Figure 5. **A**) photographs of core boxes; **B)** masked images used for the hyperspectral image processing to exclude pixels without geological information; **C)** auto-clustering map (K-means clustering with 10 classes) superimposed on the photographs.

3. SPECTRAL MAPPING

3.1 Concept of spectral unmixing

Most spectra in a hyperspectral image represent a mixture of material. The measured pixel-spectra are therefore a combination (mixture) of the different material-spectra present in the pixel. One concept in hyperspectral image analysis is to retrieve the so-called end-member spectra which represent the spectra of the spectrally purest materials, which allows to explain the spectral composition of the mixed spectra. When the end-member spectra are known, the proportion of these spectra within a pixel can be determined for all image pixels based on a commonly linear, spectral mixing model (see also Appendix C). Spectral unmixing results in score-images, one score-image per end-member, whereas the unmixing scores indicating the proportion of the respective end-member spectrum within the pixel spectra. The unmixing scores ranging between zero and one. Score zero means this end-member spectrum is not present in this pixel. Score one means that this pixel consists 100% of this end-member spectrum. The score images can be used as ***abundance maps*** **(mineral distribution maps) showing the sub-pixel concentration for each end-member material in a pixel**.

3.2 Extracting a representative set of end-member spectra

In this study the end-member spectra have been extracted from the spectral image data with a statistical method to ensure spectrally purest representations, particularly in the fine-grained material. To ensure a representative set of end-member material, the mafic gneiss end-member has been measured from an area with known lithology. The locations, where in the core the end-member spectra have been extracted, are shown in figure 8, together with the XRD sample positions. Since rocks consist of a mixture of minerals and particularly due to the small grain sizes of clay minerals, the end-member spectra might represent to some extent, mineral mixture, and not necessarily pure minerals. The name-given mineral is the dominate mineral phase in this end-member spectrum, however other minerals might be present. Six end-member spectra have been found to be representative of the analysed core boxes (Figure 6) with a focus on the clay mineral composition.

3.3 Interpretation of end-member spectra for mineral composition

The mineral composition of the end-member spectra (Figure 6) have been interpreted based on diagnostic absorption properties and by comparison with the USGS spectral library (Clark et al. 1993).

Naming of the end-member spectra

The names of the end-member spectra start with a unique number (#-number) used as ID during processing to administrate a larger number of end-member spectra. The mineral names are descriptive and based on the spectral interpretation only. End-member spectra which might be dominated by feldspar or quartz have been indicated with question marks because these minerals do not provide diagnostic absorption properties within the measured spectral rage to reliably interpret the presence of these minerals from the spectral properties alone.

#1 cryptocrystalline quartz (?)

This spectrum is, at present stage, difficult to interpret based on the spectral properties alone without additional knowledge about the mineral / chemical composition. The spectrum comes from a c.2cm thick “layer” in box 5 (box-section 3) at c.948.3m core depth. This 2cm thick section gets highlighted by many spectral products. The very pronounced absorption at 1470nm has not been observed in any other spectrum elsewhere in the core boxes. However, the absorption at 1415nm and 2230nm might indicate the presence of clay minerals. The wide absorption at 1900nm indicates presence of water molecules and the shape of this feature, might indicate intracrystalline water in quartz. Two more absorption features occur at 2280nm and 2360nm.

#6 chlorite

This spectrum shows absorption features at 1393nm, 1915nm, 2251nm, 2323nm, 2385nm and an inclined curve shape between 1100-1900nm. The absorption features and the curve shape indicate that this spectrum is dominated by chlorite.

#13 calcite

In this spectrum, diagnostic carbonate absorption features occur at 1875nm, 1994nm, 2155nm and 2336nm. The exact wavelength positions of these carbonate absorption features revealing the carbonate as calcite.

#22 smectite

This spectrum shows pronounced absorption at 1415nm and 2211nm caused by hydroxyl ions and at absorption at 1909nm caused by water molecules. The wavelength positions and the slightly asymmetrical V-shapes of these absorption features are diagnostic of smectite.

#32 altered feldspar (?)

This spectrum is, at present stage, difficult to interpret based on the spectral properties alone without additional knowledge about the mineral / chemical composition. Despite absorption features at 1443nm, 1931nm and weakly at 2195nm the spectrum is relatively flat and show similarities to felspar spectra in the USGS spectral library (Clark et al. 1993). Absorption at 1400nm and 2200nm due to hydroxyl ion and absorption at 1900nm due to water are typical of clay minerals. However, the wavelength positions and shapes of these absorption features in this spectrum differs slightly from typical clay features. It is possible that the atypical clay features are caused by mixing effects. Since this spectrum is measured in the middle of a feldspar grain it is interpreted as altered feldspar.

#500 mafic gneiss

The statistical method for the spectral end-member extraction has not found an end-member spectrum within the mafic gneiss. Therefore, a mafic gneiss spectrum has been measured in box 3 (box-section 5) at c. 769.2m core depth. This spectrum is flat without absorption features, which is typical of quartz and feldspar rich material, but can contain also other minerals with featureless spectral curves within the VNIR and SWIR spectral range.

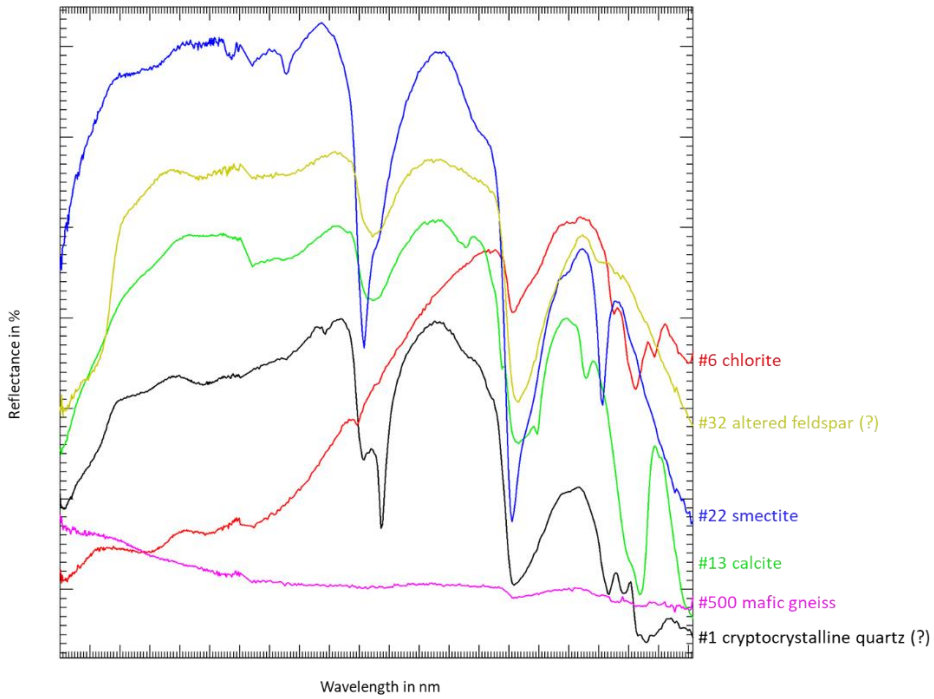

Figure 6. Representative set of end-member spectra extracted from the spectral image data.

3.4 Mapping distribution of spectral end-members

To map the distribution of the material represented by the end-member spectra shown in figure 6, linear spectral unmixing has been applied using Mixture Tuned Match Filtering (Boardman and Kruse, 2011). Figure 7 shows the spectral unmixing result and provides distribution maps of the end-member materials. The digital values shown in these spectral maps are unmixing scores ranging between zero and one and represent the proportion of the respective end-member spectrum in the pixel spectra. Value zero means that none of the end-member spectrum is present in the pixel-spectra. Value one means that the pixel spectra consist of 100% of the respective end-member spectrum. **The unmixing scores can be considered as material abundance (mineral concentrations) within the pixels.** Instead of showing the scores as grey-scale images, the scores are visualised in a simplified manner by subdividing four score-ranges to represent the scores with 5 colour classes and to indicate if an end-member material is “non” or with “very low”, “low”, “medium” or “high” abundance (concentration) present in the pixels. Note that the colour classes are not equally divided. The class deviation is indicated by the colour bar below the histogram of the unmixing-scores. These spectral maps provide **spatial information**, showing where in the core the respective material is present and provide **quantitative material information** in terms of **i) how many pixels contain the respective material** and **ii) what is the sub-pixel abundance (concentration) of this material.**

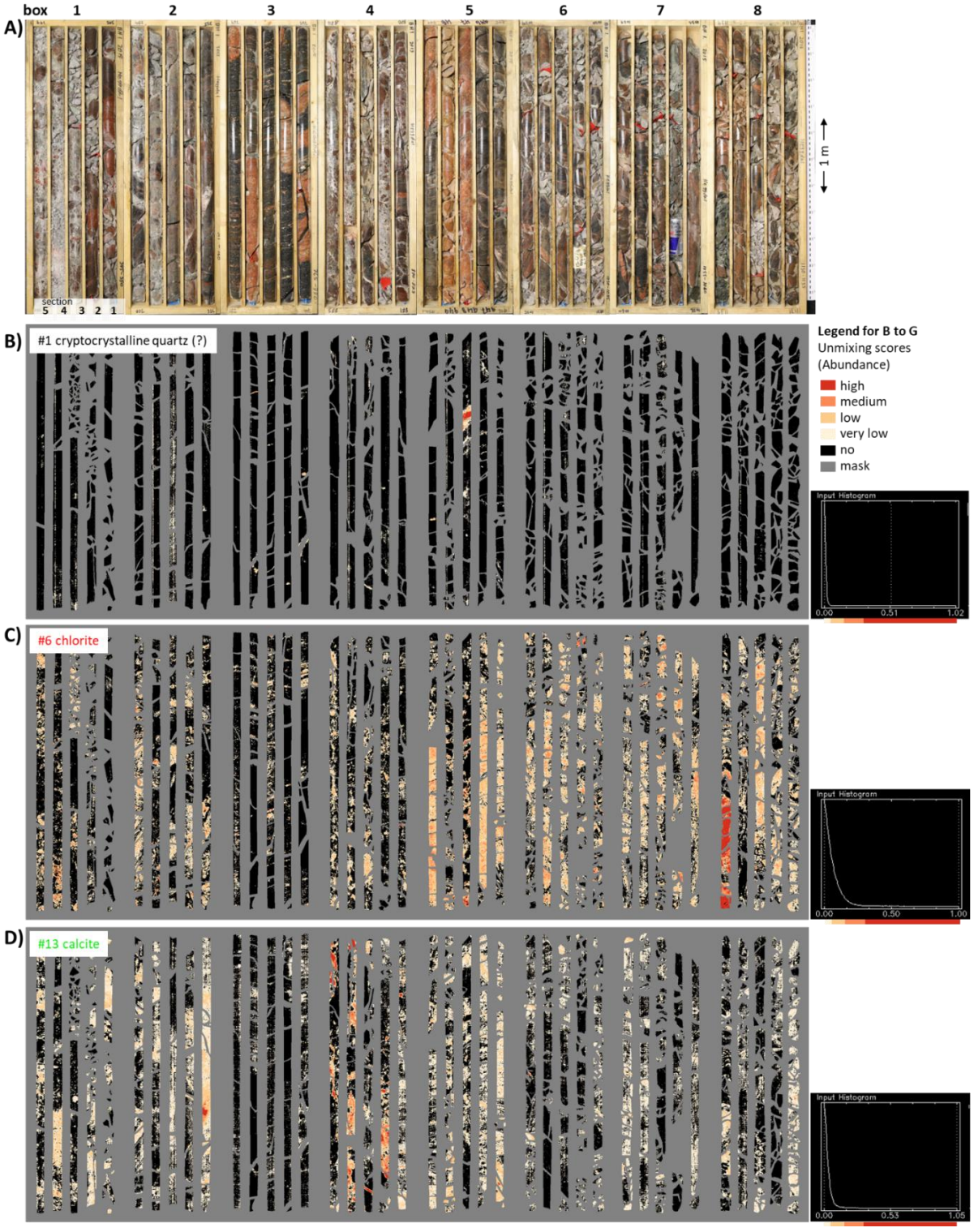

See next page for figure caption.

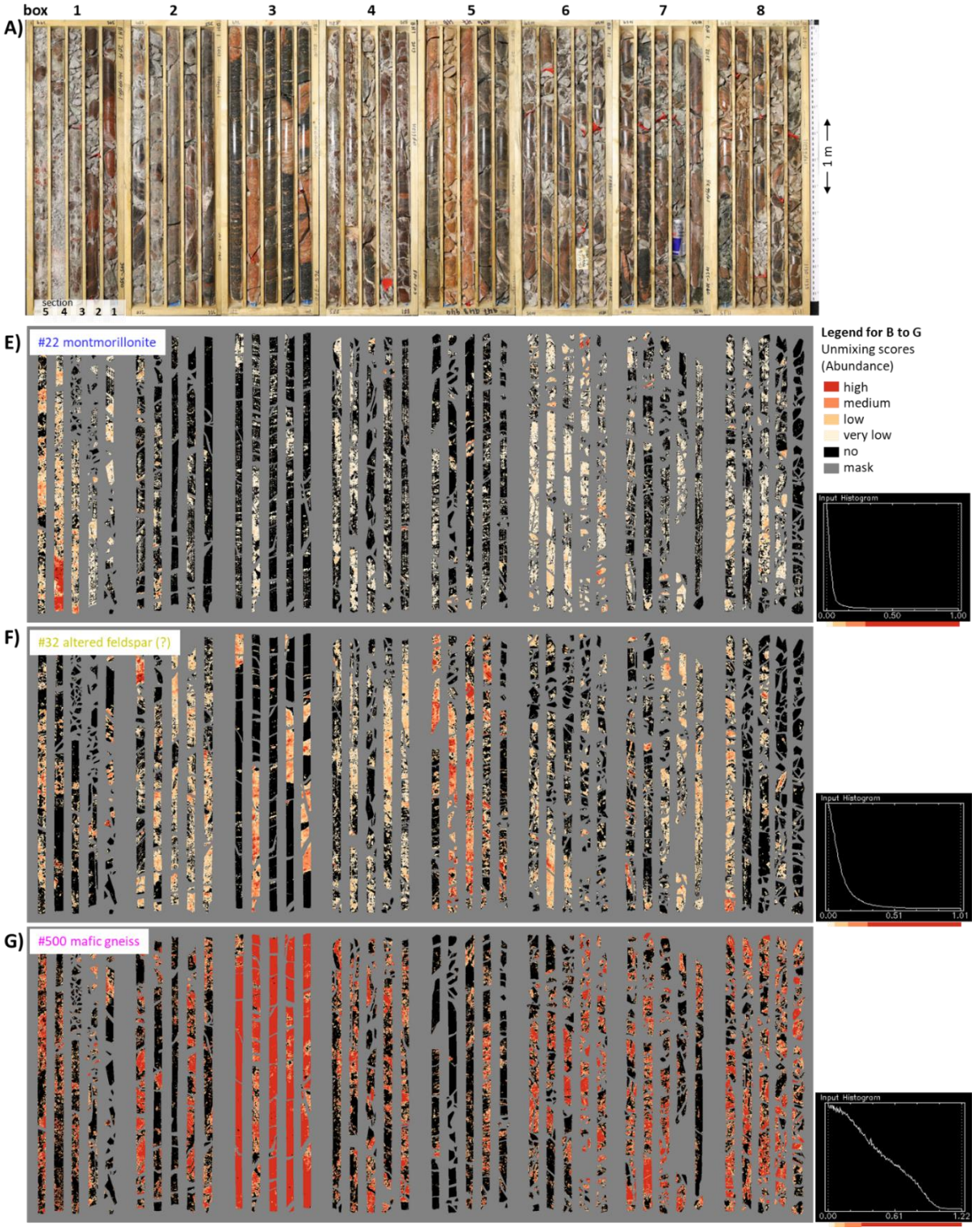

Figure 7 (split over 2 pages). Photographs and **abundance maps (mineral distribution maps)** for the end-member materials **A)** core-box photos, **B**) #1 cryptocrystalline quartz, **C)** #6 chlorite, **D)** #13 calcite, **E)** #22 smectite, **F)** #32 altered feldspar, and **G**) #500 mafic gneiss. Histograms of the score values are shown for better understanding of the visualisation. The class deviation is indicated by the colour bar below the histogram of the unmixing-scores.

4. XRD SAMPLE ANALYSIS

Sample analysis for mineral composition supports and complements hyperspectral studies and helps to explain spectral signatures such as the end-member spectra and to confirm spectral mapping results. Although XRD analysis was not a part of the project agreement, five samples have been chosen for bulk mineral analysis with XRD using the laboratory facilities and analyse routines at NGU (Table 3, Figure 8). Positions of samples #125351 and #125454 have been chosen to confirm the mineral composition of the end-member spectra which have been interpreted to contain clay minerals with swelling potential. The other three NGU samples have been taken to check the spectral mapping results. According to XRD analysis, sample #125354 comprises smectite intercalated with chlorite forming a mixed-layer clay. In that case, only the sum of “pure” chlorite (chl) and chlorite-smectite (chl-sm) can be given due to limitations in modelling. When no mixed-layer clays were identified, quantification is given for “pure” smectite and “pure” chlorite. Sample #125323 is showing a white material in fracture infills. The mineral composition of this white material has been analysed qualitatively with a separate XRD analyses. Smectite, chlorite, calcite quartz and plagioclase have been identified.

Two more sample analysis are available from the master-thesis Rødal et al. (2016). These samples have been analysed at NTNU/SINTEF with XRD and swelling parameters have been measured (Table 4, Figure 8). The parameter of the XRD analysis remain bit vague. It is not clear if the XRD results provides bulk mineral analysis or if the grain size fraction below 60µm (as stated in the text in the master-thesis) or grain size fraction below 20µm (as stated in the tables in the master-thesis) has been analysed. Smectite has been analysed only qualitatively and has not been quantified. Both samples have been also analysed for swelling pressure and free swelling. However, sample 3 did not provide enough material in the finer grain size fraction to measure swelling parameters.

Figure 8. show the sample positions for XRD analysis as well as the positions of measurements of the end-member spectra. When comparing XRD and hyperspectral results, mineral composition might differ slightly due to the different nature of methods. With hyperspectral imaging, composition at surfaces is measured, through at the highest resolution of c.1mm^2 when a single pixel is measured. In contrast, XRD measures the mineral composition from a volume and the sample material is removed from areas commonly larger than a centimetre. It is impossible to perform the spectral and XRD measurements from exact the same area / sample material. The NTNU samples have been removed before the cores have been scanned with HSI. Spectra for these samples have been measured beside the XRD sample spots.

Table 3. XRD analysis at NGU, mineral concentrations in weight%

NGU-nr	sample ID core depth	qtz	K-fsp	plag	cal	dol	ill/musc	bt	chl	chl and chl-sm	sm	tlc	amph	*GOF**	*Rwp**
125351	348.88m	42	12	19	8				spor		16	3		*3.19*	*14.17*
125352	347.64m	44	19	13	3	spor	5		2		12	2		*2.87*	*12.31*
125353	*947.80m*	*31*	*25*	*35*	*6*		*spor*		*3*		*spor*			*4.68*	*22.32*
125353	*white crust In fractures*	*sm, little chl, much cal, qtz, plag*													
125354	1134.74m				16			37		25			22	*5.05*	*15.36*
125355	1132.80m	28	18	43	spor		3		5		3			*2.94*	*12.11*

*GOF and Rwp indicating reliability of the Rietveld modelling.
GOF <2.5: very good modelling; GOF <3.0: reliable modelling
Smaller GOF and Rwp values indicate more reliable model fit (simplified phrased).

Abbreviations XRD analyse, NGU

qtz	quartz	chl	chlorite group
K-fsp	alkali feldspar	chl og chl-sm	chlorite and chlorite-smectite mixed layers
plag	plagioclase	sm	smectite group
cal	calcite	tlc	talc
dol	dolomite	amph	amphibole
ill/musc	illite / muscovite	GOF	goodness of fit
bt	biotite	Rwp	weighted profile factor

Table 4. XRD analysis at NTNU / SINTEF of samples 3 and 4 from Rødal (2016)

Sample no. in Rødal (2016)	sample 3	sample 4
fraction material <20µm	2 %	9 %
swelling pressure	N/A	0.27 MPa (intermediate active)
free swelling	N/A	160 % (highly active)
swelling minerals (smectite)	Ja (clear spike in XRD)	Ja
alkali feldspar	33 %	20 %
mica minerals	21 %	6 %
chlorite	16 %	32 %
zeolite	14 %	
quartz	9 %	26 %
pyroxene	5 %	2 %
plagioclase	<1 %	14 %
calcite	<1 %	

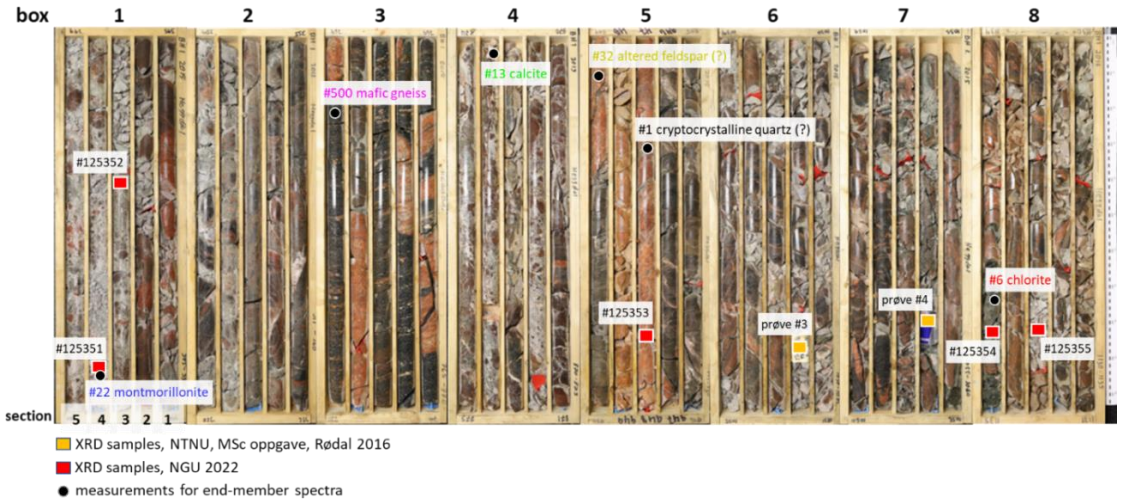

Figure 8. Sample positions for XRD analysis and positions of measurements for the end-member spectra.

Spectral measurements from XRD sample spots

Figure 9 shows the spectra measured at the XRD sample spots. The spectra are averaged over few image pixels.

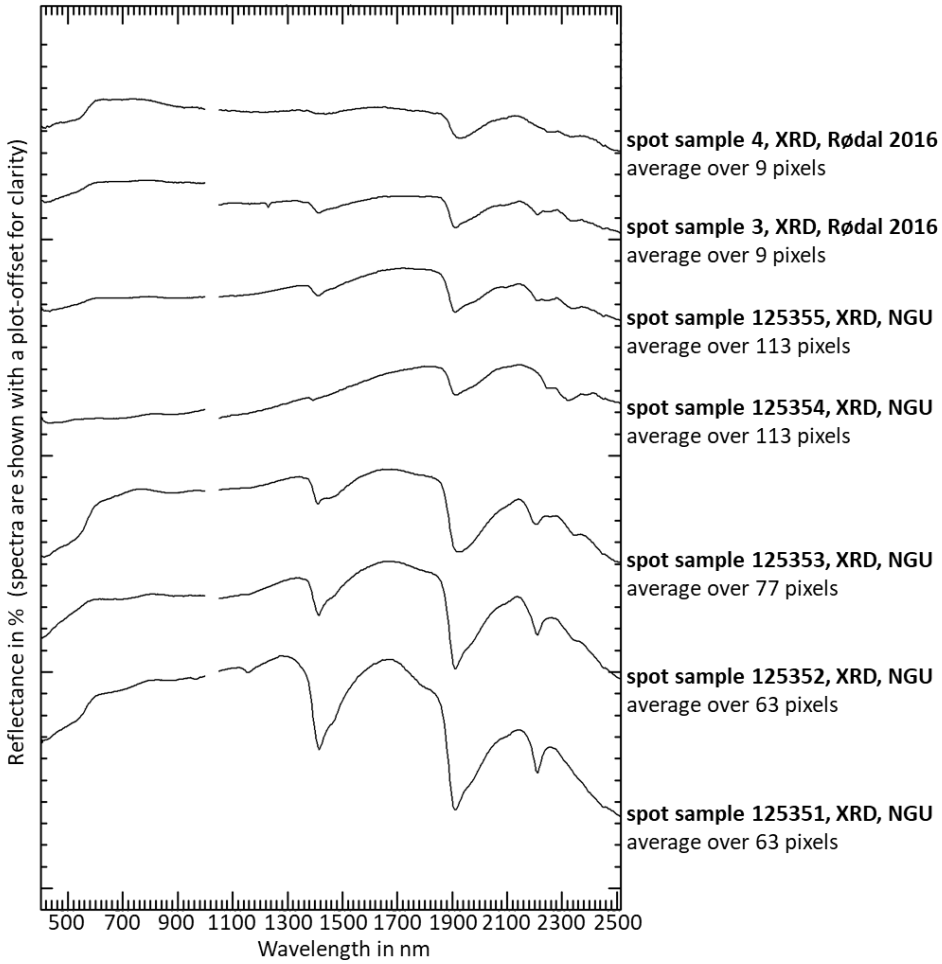

Figure 9. Spectra measured from the spots (few mm in sizes) within the boxes where the samples for the XRD analysis have been taken.

spectrum spot sample #125351, NGU

This spectrum shows diagnostic spectral properties typical of smectite with the deepest clay absorption compared to the spectra of the other sample spots. Comparison with the USGS spectral library (Clark et al. 1993) shows high similarity to montmorillonite reference spectra. The XRD analysis characterises this sample with together 73wt% quartz and feldspar and 17wt% clay whereas the clay consists of smectite with traces of chlorite. The XRD analysis confirms that the end-member spectrum from this spot represents the highest smectite content and provides therefore a god measurement for “spectrally purest” smectite. It should be also noted that the spectrum shows a smectite signature although the smectite content is not more than 17wt% in the XRD sample.

spectrum spot sample #125352, NGU

This spectrum shows diagnostic spectral properties typical of smectite, however the absorption depth is less compared to the spectrum from sample spot #125351. Comparison with the USGS spectral library (Clark et al. 1993) shows high similarity to montmorillonite reference spectra. The XRD analysis shows similar quartz and feldspar content (together 76wt%) as for the sample spot #125351. The smectite concentration with 12wt% is slightly lower. The mineral content is slightly

more divers compare to the sample spot #125351. The spectral map predicts smectite for this spot but with low and medium abundance. The XRD analysis confirms this prediction.

spectrum spot sample #125353, NGU

This spectrum shows spectral absorption due to hydroxyl-ions and water but with moderate absorption depths. Comparison with the USGS spectral library shows some similarities to feldspar and quartz reference spectra. The spectral map predicts high amount of the “altered feldspar” material at this sample spot. The XRD analysis confirms a high feldspar concentration with small concentrations of different clay types (illite/muscovite, chlorite, smectite). The XRD analysis indicates that the white material from fracture infills contains smectite, chlorite and calcite. This explains that these materials have been spectrally mapped with low abundances in isolated pixel clusters within the brecciaed, red-coloured gneiss in this core section.

spectrum spot sample #125354, NGU

The spectrum shows absorption features at 1393nm, 1909nm, 2251nm and 2323nm which are diagnostic for chlorite. Comparison with the USGS spectral library (Clark et al. 1993) shows similarities to corrensite. Corrensite is a clay consisting of 1:1 regular interstratified chlorite and smectite layers. The XRD analysis indicates that chlorite and smectite occurs as mixed layer clay in this sample. The sum of smectite and chlorite-smectite is 25wt%. Since this spectrum shows a strong chlorite signature it indicates that chlorite is most likely the dominant clay type in this sample. The XRD analysis supports the interpretation that the end-member spectrum “#6 chlorite” measured at this spot represents the highest chlorite content. This spot provides therefore a god measurement for “spectrally purest” chlorite. However, XRD reveals also that some smectite is presence in the form of chlorite-smectite mixed layer clay.
The XRD analysis indicates also 37wt% biotite. Since biotite does not possess expandable properties, the identification and mapping were not in focus in this study. More work is required to adjust the spectral mapping methods for a wider range of minerals such as biotite.

spectrum spot sample #125355, NGU

The spectrum shows absorption features at 1410nm, 1909nm, 2211nm and 2239nm and 2335nm and 2452. These spectral features indicate that this spectrum contains smectite and chlorite whereas smectite might be dominating. The XRD confirms the present of chlorite but with lower concentrations compared to sample spot #125354. The spectral map predicts smectite and chlorite for this spot, both materials with pixels indicating low and medium abundance. The XRD analysis confirms this prediction.

sample 3 and 4 in Rødal 2016, NTNU/SINTEF

The spectral maps indicating, in the neighbourhood of these sample spots, the present of smectite and chlorite with mostly low sub-pixel abundances. The XRD analysis confirms the present of smectite and chlorite at these sample spots.

5. SPECTRAL MAPPING RESULTS

This prove-of-concept study focuses on the spectral mapping of clay material with swelling potential within the Heggdal KBH1 core. A more extensive spectral mineral mapping requires more time to adjust the spectral mapping methods to the other relevant minerals such as biotite, muscovite and others. The evaluation of the hyperspectral images shows that image spectra with smectite and chlorite signatures have been found. The smectite and chlorite signatures have been confirmed by XRD analysis. The chlorite can occur in mixed layer clay together with smectite. Swelling potential can be therefore expected in smectite and chlorite bearing material in theses cores.

According to the hyperspectral analysis the clay materials in this core material seems to be dominated by smectite and chlorite but also carbonate material can be present. This spectral observation has been confirmed by XRD sample analysis. Spectra dominated by illite/muscovite have been, at this processing stage, not observed. However, XRD indicates small concentrations of illite/muscovite. More work is required, applying more sophisticated processing to test if such

small illite concentration can be extracted and mapped from the hyperspectral image data. No spectral indication has been found for kaolinite. The absents of kaolinite has been confirmed by XRD sample analysis.

The highest concentration of smectite have been found in box 1 (box-section 3 to 5) between core depth 347.4-350.00m whereas the material between 348.65-349.00m (bottom of box section 4) shows spectrally highest purity of smectite. This core section might provide a representative sample location to determine the swelling potential. The hyperspectral maps indicate that smectite seems to be widespread in these cores, through with low concentration. Core boxes 6 and 7 seems to have a high number of pixels with smectite with very low to low abundance (concentration).

The highest concentration of chlorite has been spectrally indicated in box 8 (bottom of box-section 5) between core depth 1134.65-1135.00m. This might be another location where swelling potential should be tested. The hyperspectral maps indicate that chlorite seems to be widespread in this core material. Core boxes 5 to 8 show a high number of pixels with very low to medium spectral abundance (concentrations) of chlorite material.

Furthermore, spectra with distinct carbonate signature have been observed. The carbonate material can be spectrally determined as calcite and has been confirmed by XRD analysis. Spectrally highest calcite concentrations have been found in box 4. The hyperspectral maps indicate that calcite seems to be widespread in this core material through with low concentrations and can be distributed in the clay rich material or occurs as fracture infill.

Although the spectral range of this data set is not optimal for detailed spectral analysis of quartz and feldspar, impurities and alteration can cause differences in spectral signatures and seems to allow the differentiation between felsic and mafic lithology. Spectrally conspicuous material, termed and interpreted in this study as “cryptocrystalline quarts”, have spectrally identified and mapped in box 5 (box-section 3) at core depth c.948.3m. Few more grains (or particles) in the core seems to have a similar spectral signature and might consists of the same material. Spectra from feldspar within the brecciated pegmatitic gneiss for example in box 3 and 5 showing spectral properties which can be eventually explained by alteration processes which can result in very fine-grained alteration products such as sericite. The spectral maps showing that the fracture infill within these brecciated gneisses consist of calcite, chlorite and smectite which was confirmed by the XRD analysis.

6. CONCLUSIONS AND FINAL REMARKS

This pilot study demonstrate that hyperspectral imaging has the potential to identify and map clay minerals with swelling potential. The same method is applicable to different mineral problems in infrastructure projects. Other hazardous materials that cause challenges due to environmental, health or economic impact are for example sulphides and sulphates (acidic rocks) or high silicate content. HSI as innovative method for mineral identification has the potential for cost savings in infrastructure projects and provides several benefits such as:

- Proving continuous mineral information of the entire core length (not possible with XRD sampling alone).
- Fast turnarounds when the processing workflow is once established (nearly in-time mineral information).
- Highlighting mineral trends over the core length.
- Ensure more representative and efficient sampling for analysis of geoengineering, geochemical and geophysical rock properties.

Follow-up projects should include further developments such as:

- Improving the automation of the processing and data evaluation.
- Testing and establishing efficient processing methods such as machine learning and deep learning approaches.
- Developing meaningful mapping products and visualisation tools for the end-users.
- Conducting confirmation studies to determine uncertainties and confidence of spectral mapping products.

SVV and NGU have confirmed the intention of closer cooperation (contract from 15.05.2023). Innovative digital mapping methods such as hyperspectral imaging of core material provide new opportunities to characterize geological weakness-zones in infrastructure projects. NGU provides expertise in both subjects, i) basement fracturing and weathering in Norway, and ii) core hyperspectral imaging, with years of experiences and extensive and unique competences. NGU suggests therefore to initiate a follow-up project and long-term cooperation on these subjects. NGU is open and highly interested to discuss further cooperation and projects on this matter.

7. APPENDIX

The appendices provide additional material which was out of scope for this report to explain and discuss in more detail. **Appendix A** provides more detailed information about the spectra diversity per core box. This highlights the potential of core HSI and demonstrates what spectral details can be observed and analysed. **Appendix B** briefly outlines the normalization of spectral curves for detailed spectral analysis. **Appendix C** provides a brief demonstration of spectral mixing.

7.1 Appendix A

Spectral diversity per core box

To get an overview of the spectral diversity, each core box has been initially analysed separately and spectra of different lithologies have been measured (Figures 10-17). The measured spectra have been interpreted by analysing diagnostic reflectance properties and by comparison with reference spectra from the USGS spectral library (Clark et al. 1993).

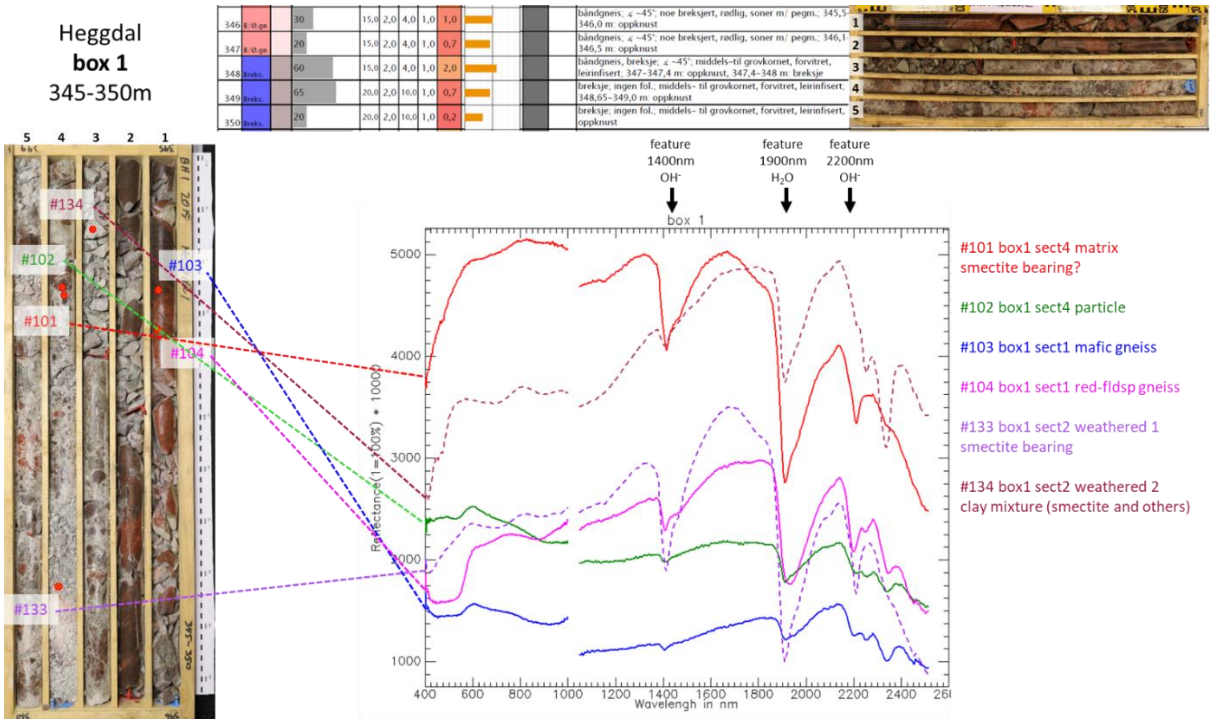

Figure 10. Spectra of different lithologies observed in core box 1. Core log at the top from Kjernelogg KBH 01 Heggdal, SVV.

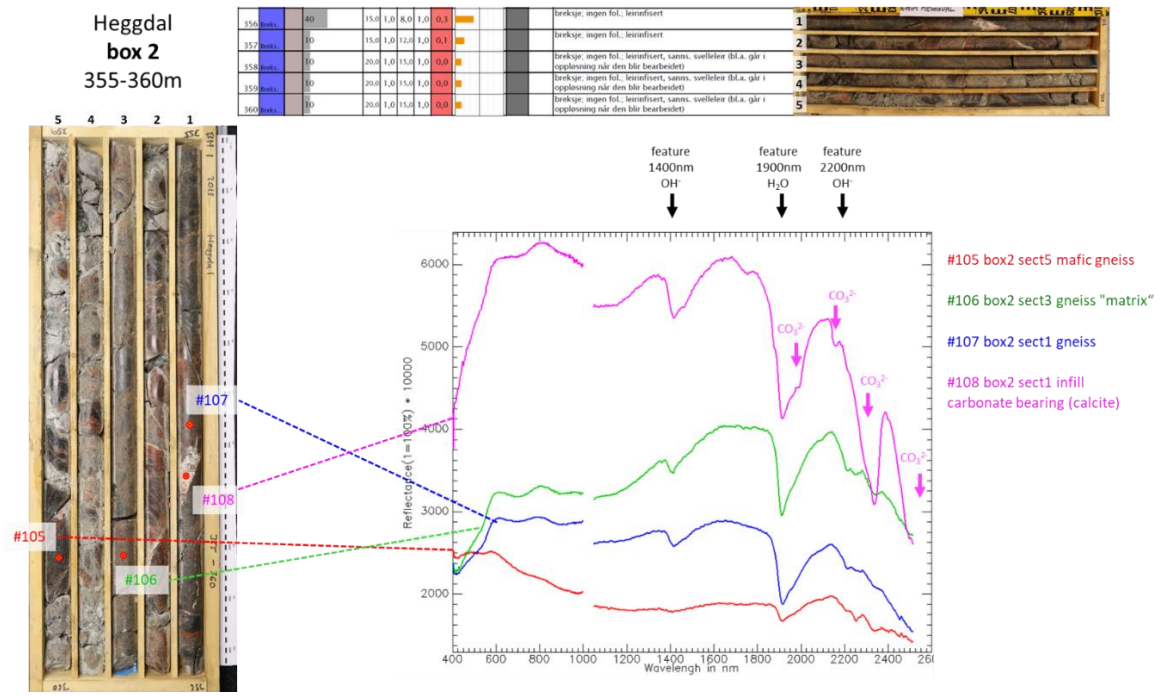

Figure 11. Spectra of different lithologies observed in core box 2. Core log at the top from Kjernelogg KBH 01 Heggdal, SVV.

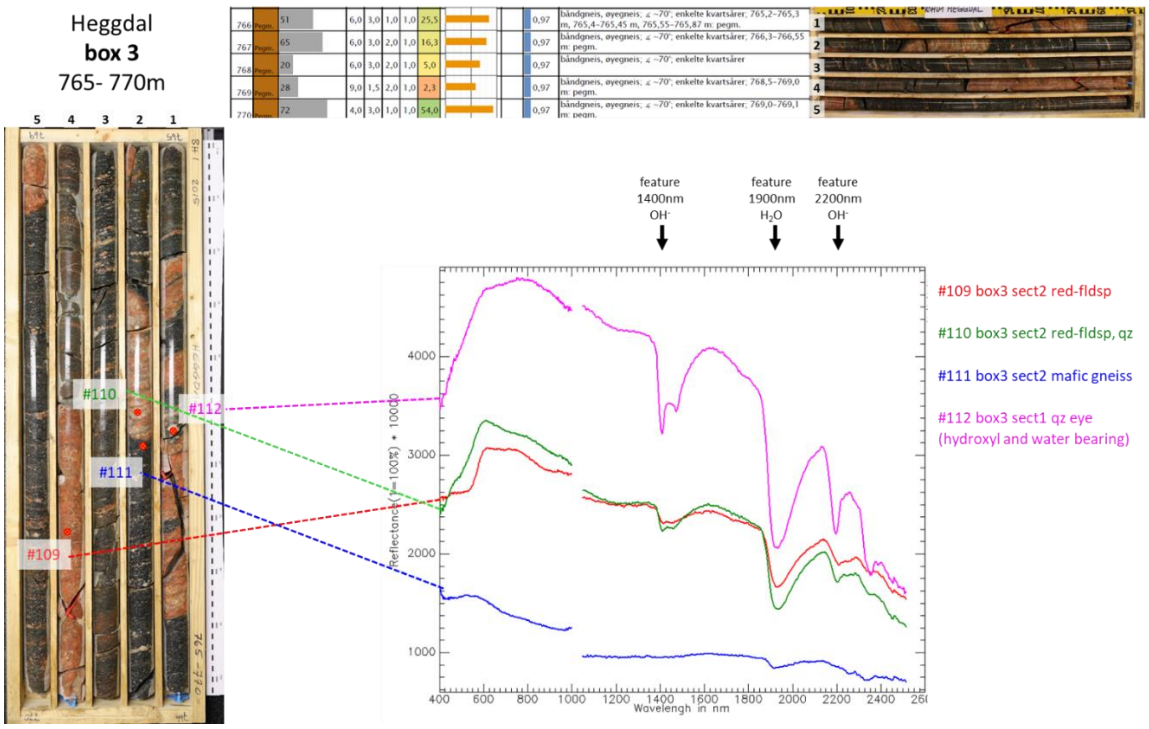

Figure 12. Spectra of different lithologies observed in core box 3. Core log at the top from Kjernelogg KBH 01 Heggdal, SVV.

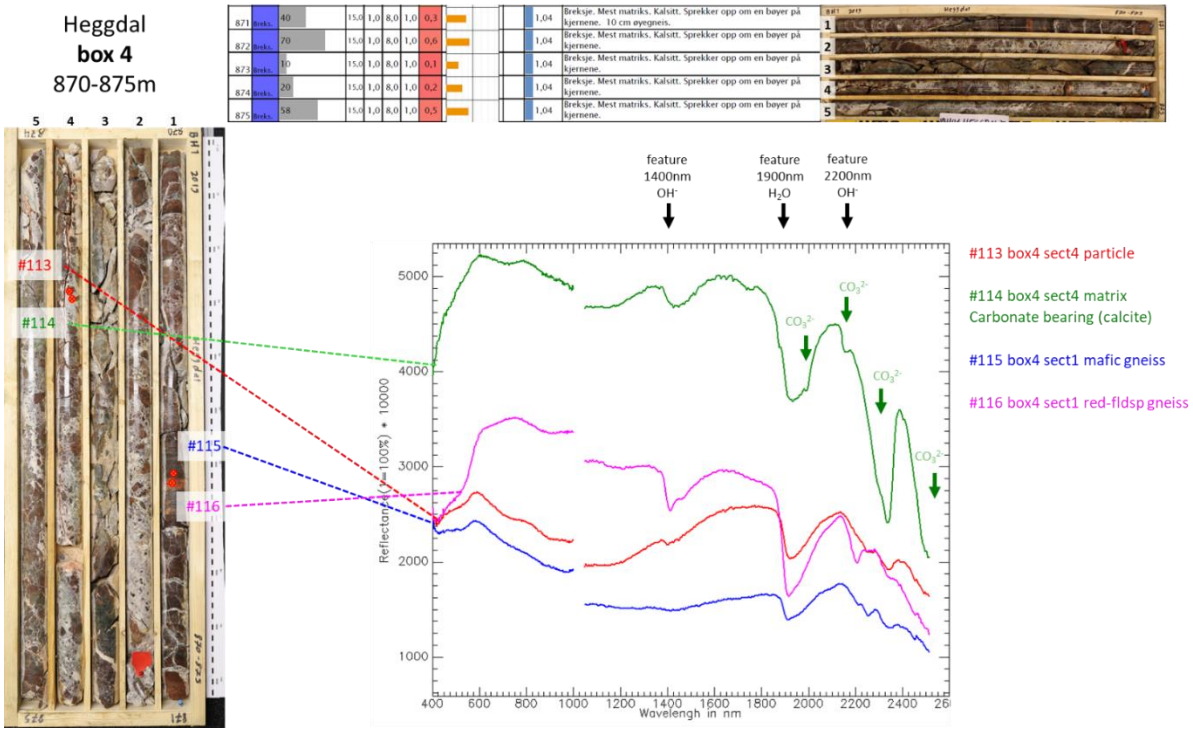

Figure 13. Spectra of different lithologies observed in core box 4. Core log at the top from Kjernelogg KBH 01 Heggdal, SVV.

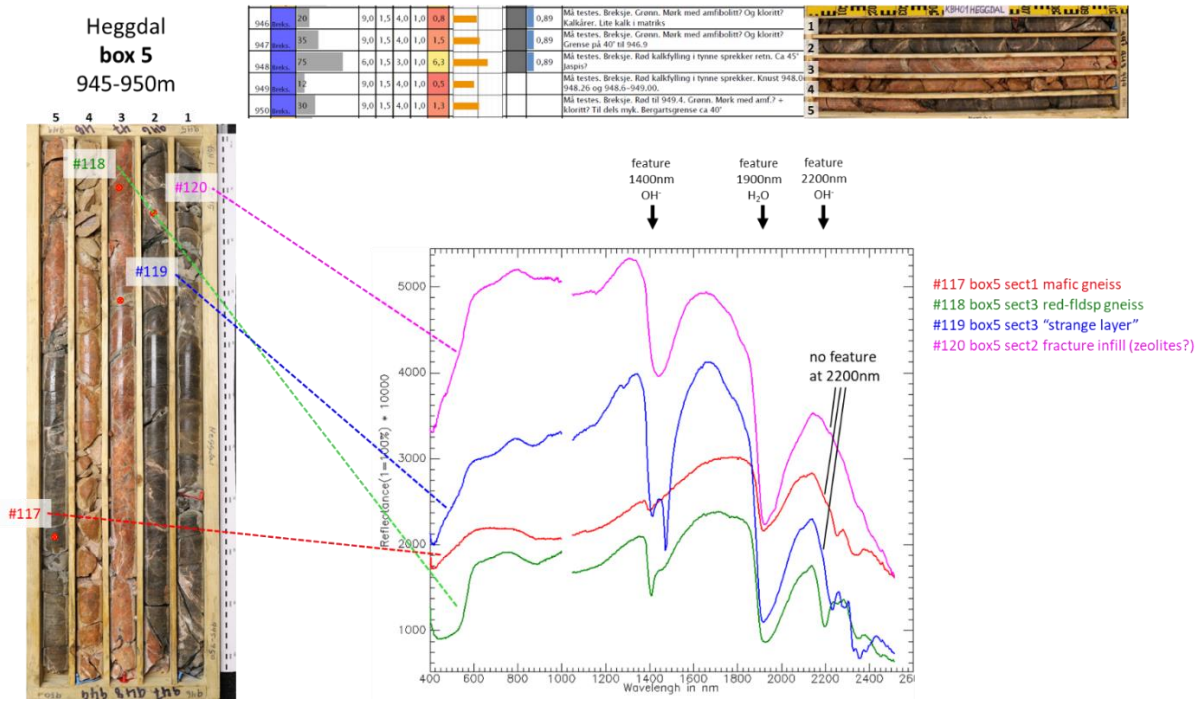

Figure 14. Spectra of different lithologies observed in core box 5. Core log at the top from Kjernelogg KBH 01 Heggdal, SVV.

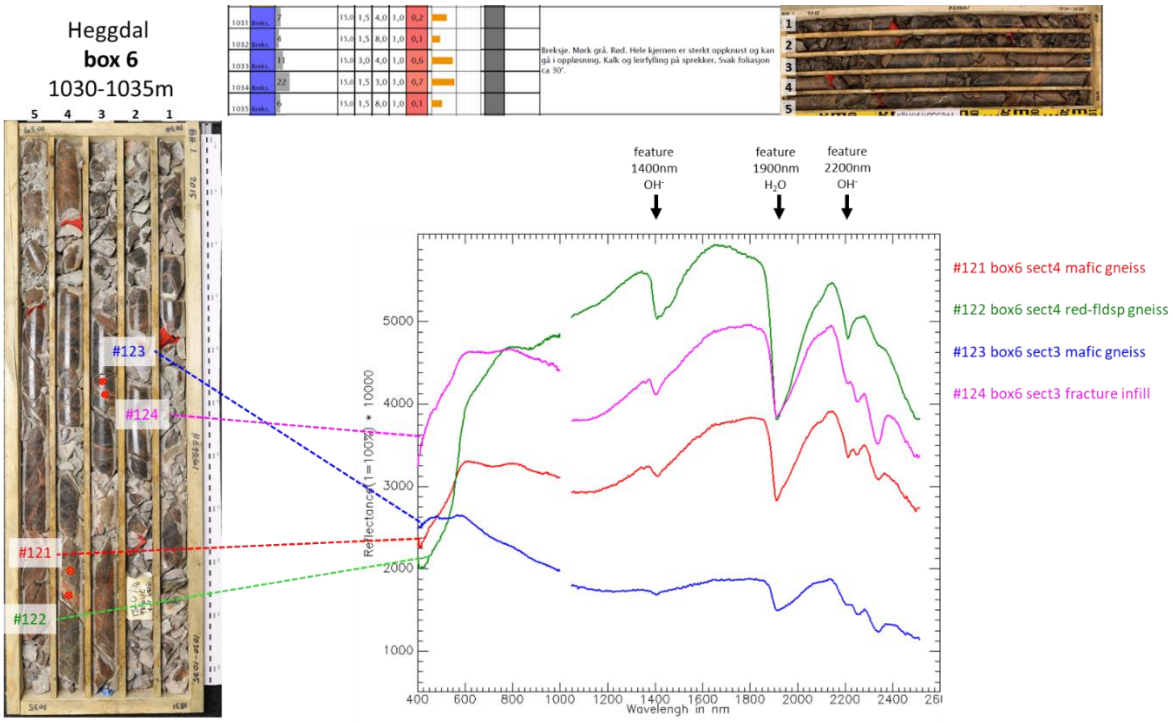

Figure 15. Spectra of different lithologies observed in core box 6. Core log at the top from Kjernelogg KBH 01 Heggdal, SVV.

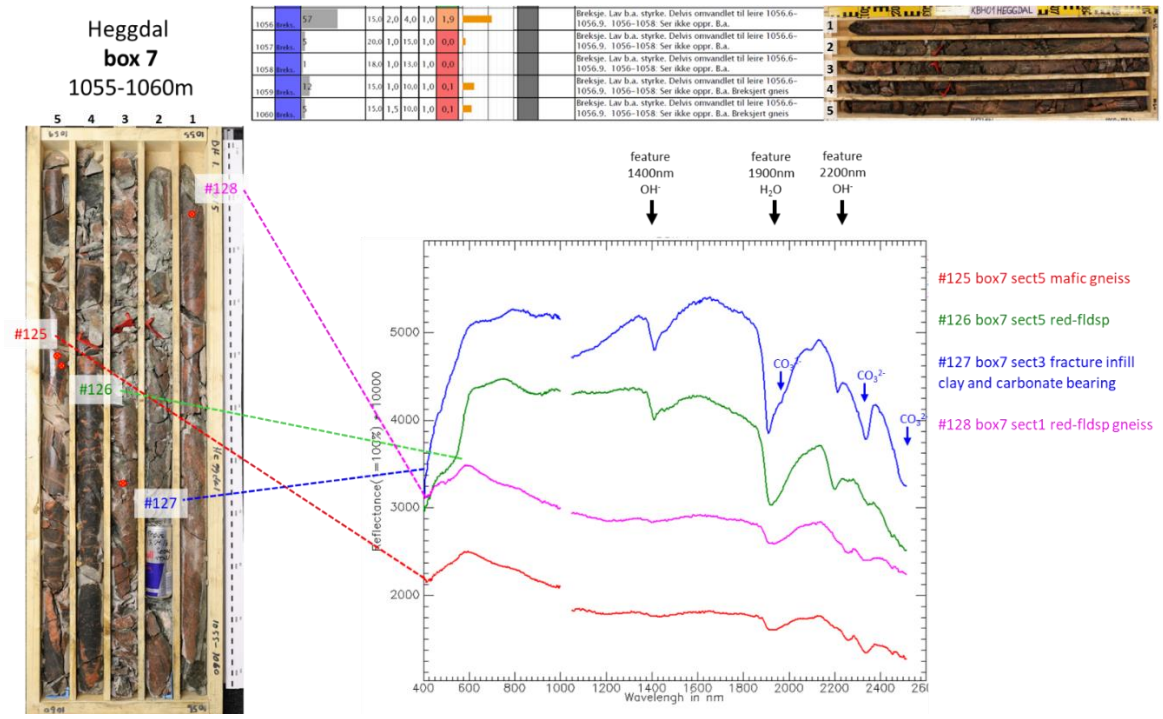

Figure 16. Spectra of different lithologies observed in core box 7. Core log at the top from Kjernelogg KBH 01 Heggdal, SVV.

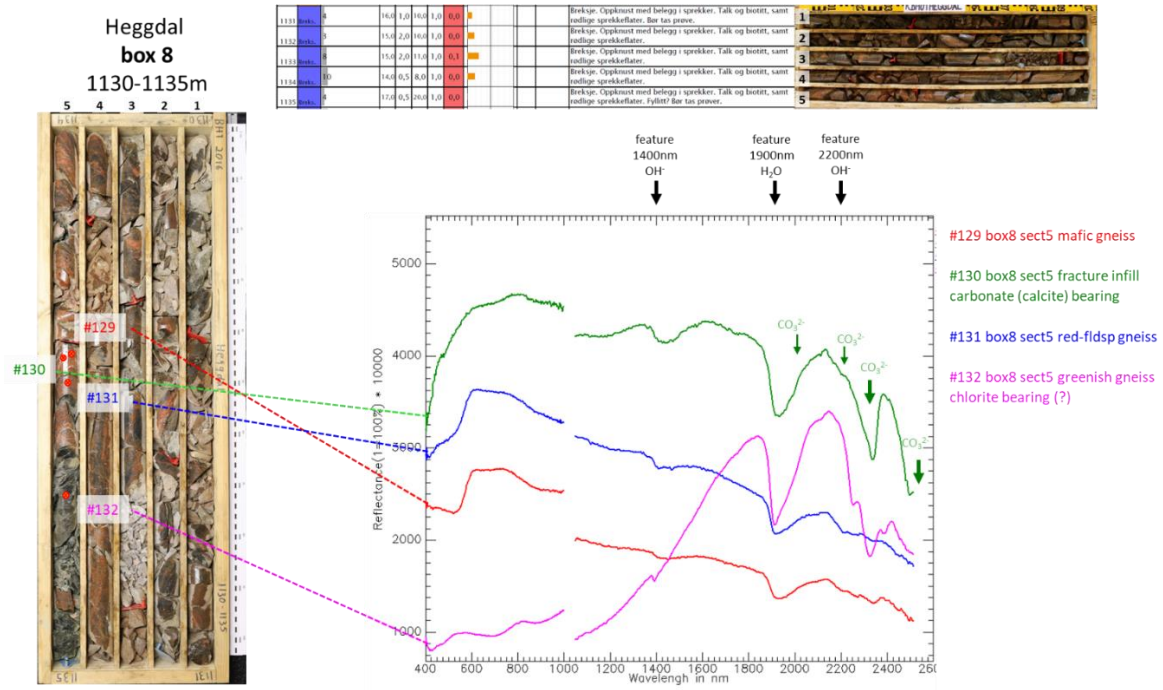

Figure 17. Spectra of different lithologies observed in core box 8. Core log at the top from Kjernelogg KBH 01 Heggdal, SVV.

7.2 Appendix B

Normalising spectra using continuum removal

For detailed spectral analysis, the spectral curves should be normalised to extract absorption features and to measure spectral properties such as wavelength positions and absorption depth. One common method in hyperspectral imaging is the continuum removal approach (van der Meer, 2004) where the convex hull of a spectrum is divided by the reflectance spectrum (Figure 18). Detailed spectral analysis in this study based on normalised spectra using continuum removal.

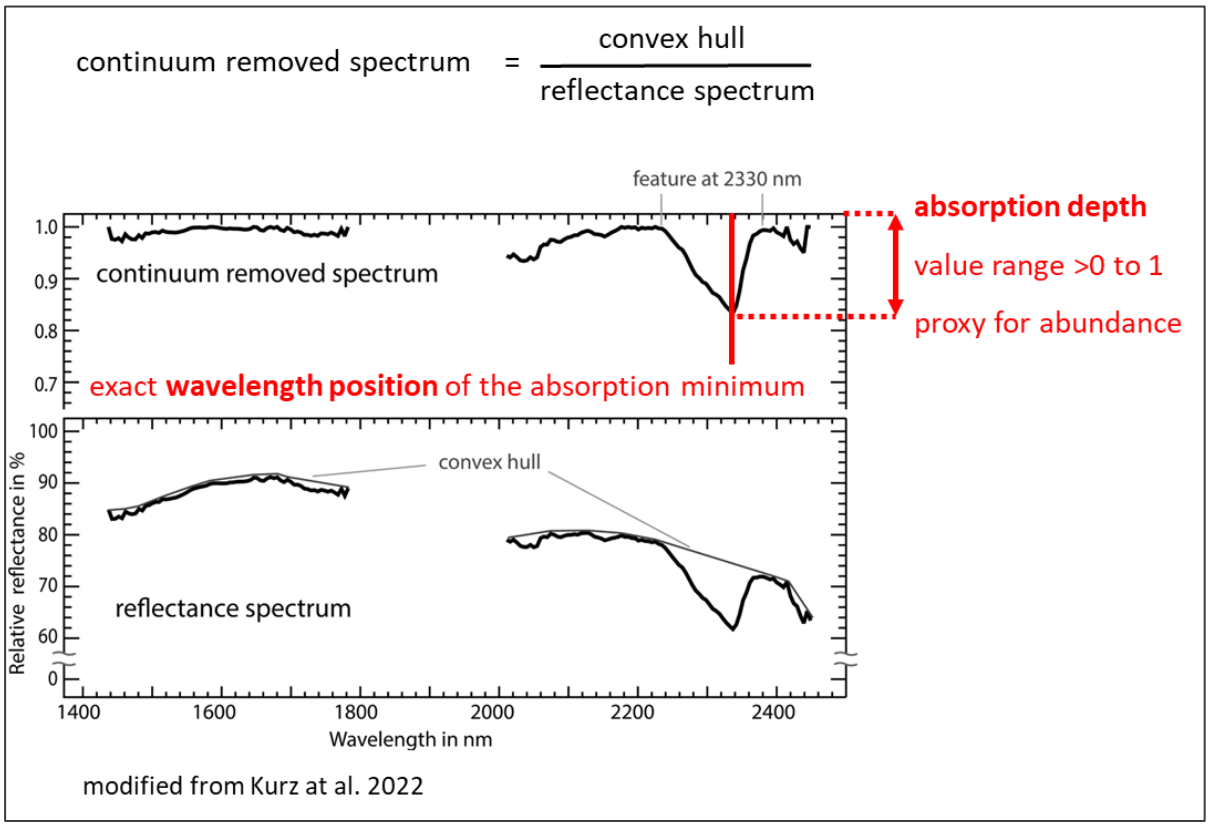

Figure 18. Normalising spectra using continuum removal to extract absorption features and to measure spectral properties such as wavelength positions and absorption depths.

7.3 Appendix C

Demonstration of artificial spectral mixing

Artificial in this context means that the spectra have been mixed mathematically. This contrasts with physical mixing by blending mineral powders together and measuring a mixed spectrum with a spectral instrument from the blended powder. Figures 19 and 20 demonstrate the concept of spectral mixing. Figure 19A and figure 20A showing four spectra of pure minerals from the USGS spectral library (Clark et al. 1993). In Figure 19B, the “mixed spectrum 1” (in red) have been generated by mixing mathematically the USGS spectra together with proportions as given in the figure (49% quartz, 17 % montmorillonite 17% illite, and 17% chlorite). The “mixed spectrum 1” is a combination of the four pure mineral spectra and combines all absorption features of the separate pure mineral spectra. In Fig 19C the spectra have been normalised to measure and compare the absorption depths of the separate absorption features. It can be clearly seen that the diagnostic absorption features in the “mixed spectrum 1” has been reduced. The absorption depths are correlated with the abundance (concentration) of the respective spectrum (material). If the components (end-members) of a mixed spectrum is known, the proportion of the individual components can be determined commonly based on a linear mixing model. Figure 20 is identical with Figure 19, but another mixed spectrum “mixed spectrum 2” (in black) is shown where quartz and montmorillonite have been mixed with 50% proportions. Such mixing experiments provides better understanding how spectra properties might change when specific minerals are mixed togethers in different proportions. This allows to adjust spectral mapping method to identify specific minerals in mixed spectra. Its also provides estimates of minimum concentration to be detectable in mixed spectra.

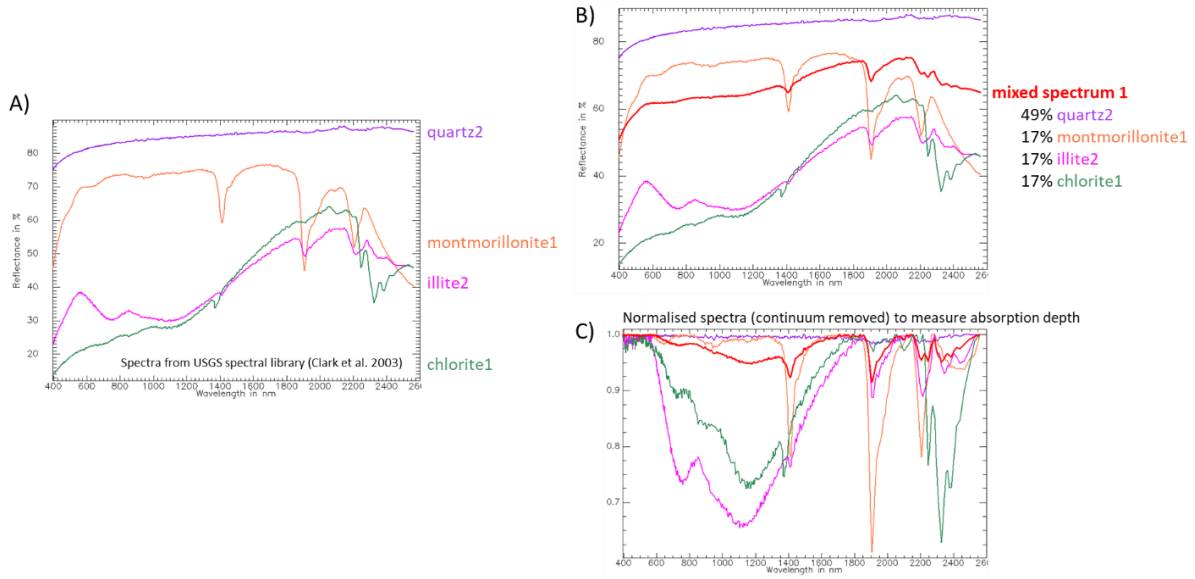

Figure 19. Demonstration of spectral mixing using a linear mixing model. **A)** Spectra from pure minerals from USGS spectral library. **B)** The “mixed spectrum 1” (in red) has been added to the spectral plot in A). The “mixed spectrum 1” has been created by mixing mathematically together the four pure mineral spectra with the proportions 49% quartz, 17% montmorillonite, 17% illite and 17% chlorite. **C)** Normalised spectra using continuum removal to measure and compare the absorption depths of the separate absorption features.

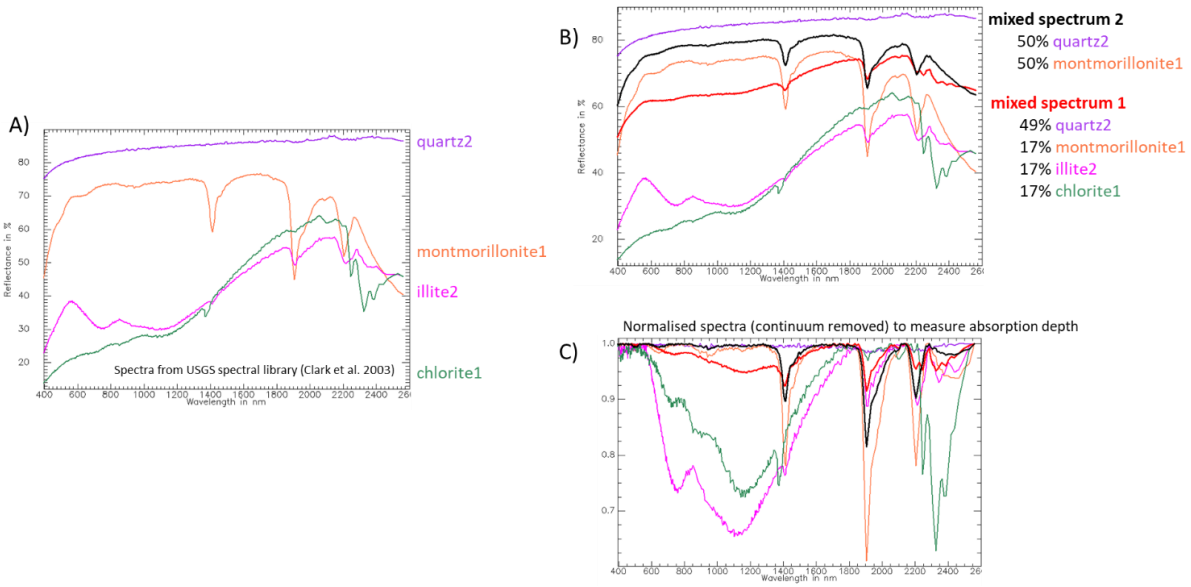

Figure 20. Demonstration of spectral mixing based on a linear mixing model. This figure is identical with figure 19 but a second mixed spectrum is shown in B) and C) where quartz and montmorillonite have been mixed with 50% proportions. (See also caption of figure 19).

References

Boardman, J.W. and Kruse, F.A. Analysis of imaging spectrometer data using N-dimensional geometry and a mixture-tuned matched filtering approach. IEEE Trans. Geosci. Remote Sens. 2011, 49, 4138–4152.

Clark, R.N., G.A. Swayze, A.J. Gallagher, T.V.V. King, and W.M. Calvin, 1993, The U. S. Geological Survey, Digital Spectral Library: Version 1: 0.2 to 3.0 microns, U.S. Geological Survey Open File Report 93-592, 1340 pages.

Kurz,T., Buckley, S., Bastesen, E., 2017. Hyperspectral Analysis of Swelling Clay. Project Report 28.11.2017, Virtual Outcrop Geology Group, Uni Research CIPR, Bergen, Norway.

Kurz, T.H., Miguel, G. S., Dubucq, D, Kenter, J., Miegebielle, V., Buckley, S. J. 2022. Quantitative mapping of dolomitization using close-range hyperspectral imaging: Kimmeridgian carbonate ramp, Alacón, NE Spain. Geosphere, 18 (2): 780–799. doi: https://doi.org/10.1130/GES02312.1

Rødal, Håkon Kjøde, 2013. Nytteverdi av styrt kjerneboring for planlegging av E39 i tunnel under Romsdalsfjorden. Master oppgave, NTNU, Institutt for geologi og bergteknikk, Trondheim, Norway, juni 2016.

Kjernelogg KBH 01 Heggdal, E136 Vik – Julbøen, Statens Vegvesen, PDF dokumenter

van der Meer F., 2004. Analysis of spectral absorption features in hyperspectral imagery. International Journal of Applied Earth Sciences and Geoinformation, v. 5, 55–68.

GEOLOGICAL
SURVEY OF
NORWAY

· NGU ·

Geological Survey of Norway
PO Box 6315, Sluppen
N-7491 Trondheim, Norway

Visitor address
Leiv Eirikssons vei 39
7040 Trondheim

Tel (+ 47) 73 90 40 00
E-mail ngu@ngu.no
Web www.ngu.no/en-gb/